Journal of Alloys and Compounds 526 (2012) 1–5

Contents lists available at SciVerse ScienceDirect

Journal of Alloys and Compounds

journal homepage: www.elsevier.com/locate/jallcom

Potassium doping effects on the structure and magnetic properties of Sr_2FeMoO_6

Y.C. Hu[a,b,*], H.X. Han[c], H.J. Hu[d], K.L. Zhang[a], H.Y. Wang[a], Y.J. Jiang[a], H. Ma[a], Q.F. Lu[a]

[a] *College of Physics and Information Engineering, Henan Normal University, Xinxiang, Henan 453007, China*
[b] *Nanjing National Laboratory of Microstructures, Key Lab of Solid State Microstructures, Department of Physics, Nanjing University, Nanjing 210093, China*
[c] *Road and Bridge Construction Co. Limited of Henan Zhongzhou, Zhoukou, Henan 466000, China*
[d] *School of Physics and Electronic Engineering, Xinyang Normal University, Xinyang, Henan 464000, China*

ARTICLE INFO

Article history:
Received 4 January 2012
Received in revised form 4 February 2012
Accepted 6 February 2012
Available online xxx

Keywords:
X-ray diffraction
Crystal structure
Vacancy formation
Magnetic measurements
Magnetoresistance

ABSTRACT

The crystal structure and magnetic properties for the ordered double perovskite oxides $Sr_{2-x}K_xFeMoO_6$ ($0 \leq x \leq 0.04$) are investigated. X-ray powder diffraction studies reveal that all the samples are single phase and have the I4/m symmetry. The anti-site defect (AS) in double perovskite oxides of $Sr_{2-x}K_xFeMoO_6$ may be adjusted by alkali metal element of K doping. The unit cell magnetization at 280 K is 1.12 μ_B for $x = 0$ and 1.26 μ_B for $x = 0.04$, respectively. The cation-ordering and the Fe—O(1)—Mo bond-angle play the competition roles on the magnetism in the doping system.

1. Introduction

Functional materials have attracted great attention in recent years due to their promising applications in wide range of device [1–5]. The double perovskite-like compound Sr_2FeMoO_6 (SFMO), with a remarkable magnetoresistance (MR) above the room temperature, has become one of the most promising candidates in magnetic storage materials [6]. SFMO is a typical ordered double perovskite structure $A_2BB'O_6$, where A is the alkaline-earth ion, B and B′ are the transition metals. As reported in [7] and [8], the crystal structure of SFMO is cubic or tetragonal, where the alternating FeO_6 and MoO_6 octahedral are arranged regularly (we call the regular arrangement as the cation-ordering) in a rock salt superlattice with the voluminous Sr cation occupying the voids among the octahedral. The existence of anti-site defects (Mo on Fe site and vice versa, AS defect) has great influence on the magnetic and transport properties of Sr_2FeMoO_6 [9–11]. The cation-ordering is believed to rely on the charge differences between Fe and Mo ions [12]. The less the difference is, the more disorder between B and B′ is. For device applications, enhancement in magnetism and capability of manipulating electo-magnetic coupling become very desirable. Chemical doping is one of effective approaches to achieve these objectives. Therefore, a technical roadmap to enhance the magnetism by either intrinsic doping or external modulation becomes attractive.

Changes of valence states in transition-metal oxides often cause significant changes in their structural and physical properties [13,14]. Chemical doping is the conventional way of modulating these valence states. In ABO_3 perovskite and/or $A_2BB'O_6$ perovskite-like oxides, chemical doping at the A site may introduce vacancies or electrons at the B site, giving rise to exotic physical properties like high transition temperature superconductivity and colossal magnetoresistance [15,16]. When two transition metals occupancy at different sites in the unit cell, they may transfer charges due to the doping. The substitution of trivalent La ions for the divalent Sr ions induces electron doping and these doping electrons inject into Mo orbit [17]. Our previous work also has demonstrated that the doping electrons reduce the valence state of Mo [18]. We report in the present on the study of the substitution of univalent potassium (K) for the divalent Sr ions in SFMO and its effects on crystal structure, valence of Fe, and resulted magnetic properties. We demonstrate that the K-doping can modulate the magnetic property, an unusual effect.

2. Experimental

Samples of $Sr_{2-x}K_xFeMoO_6$ ($x = 0$, 0.01, 0.02, 0.03, 0.04) are prepared by standard solid-state reaction. Details are given in our previous paper [19]. Briefly, stoichiometric powders of $SrCO_3$, Fe_2O_3, MoO_3 and K_2CO_3 are mixed, ground and heated at 900 °C for 10 h in air. The pre-reacted mixture is then finely ground,

---

* Corresponding author at: College of Physics and Information Engineering, Henan Normal University, Xinxiang, Henan 453007, China. Tel.: +86 373 3329037; fax: +86 373 3329037.
E-mail address: yanchunhu@htu.cn (Y.C. Hu).

0925-8388/$ – see front matter © 2012 Elsevier B.V. All rights reserved.
doi:10.1016/j.jallcom.2012.02.059

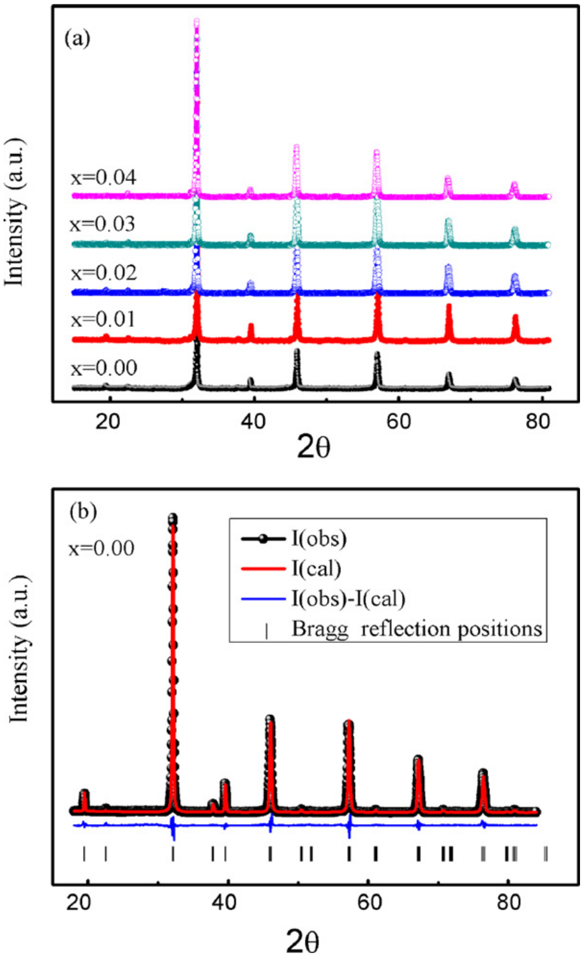

Fig. 1. (a) Measured XRD pattern for polycrystalline $Sr_{2-x}K_xFeMoO_6$ ($0 \le x \le 0.04$). (b) The Rietveld refinement for sample $x = 0$.

pressed into pellets and sintered at 1280 °C in a stream of 5% H_2/Ar gas for 15 h with several intermediate grindings. The samples are heated and cooled at a rate of 5 °C/min under the atmosphere above. Structure of the sample is examined by X-Ray Powder Diffraction (XRD) using a Rigaku D/max 2500 diffractometer with Cu Kα radiation (50 kV 120 mA) and a graphite monochromator. A step scan mode is employed with a step width of $2\theta = 0.02°$ and a sampling time of 2 s. The XRD patterns show that the samples crystallize in single phase. The XRD data is analyzed by means of the Rietveld refinement program GSAS [20]. Oxygen content in the formula is determined by the double iodometric titration, which is developed in our previous in the oxygen content determination in high-T_C superconductors [21,22]. The M–H curves of these samples are measured by a vibrating sample magnetometer (VSM). The magnetoresistance properties are measured using a standard four-probe technique with a magnetic field applied.

3. Results and discussion

Fig. 1(a) presents the laboratory measured θ–2θ XRD patterns for the samples with $x = 0$–0.04. The XRD results show that all samples crystallize in single phase with the symmetry of I4/m. In order to identify details of the structural distortion, we perform the Rietveld refinements using the XRD data collected at laboratory. The atoms occupy at: Sr/K, 4d (1/2, 0, 1/4); Fe/Mo, 2a (0, 0, 0), (denote as B-site); Mo/Fe, 2b (0, 0, 1/2), (denote as B′-site); O1, 8 h (x, y, 0); O2, 4e (0, 0, z). Before refinements, we assume full occupancy for each site in the unit. During refinements, the real occupancy maybe change according to the difference between the measured XRD patter and the calculated one. The weak scattering of oxygen on X-ray may result in the insensitive to the XRD intensity, thus oxygen occupancies are assumed to the values determined from the double iodometric titration measurement. The values for all samples are nearly 6 due to the oxygen is rich throughout the preparation ($x \le 0.04$), where the reaction is:

$$(8-4x)SrCO_3 + 2Fe_2O_3 + 4MoO_3 + 2xK_2CO_3 \rightarrow 4Sr_{2-x}K_xFeMoO_6 + (8-2x)CO_2\uparrow + (1-x)O_2\uparrow$$

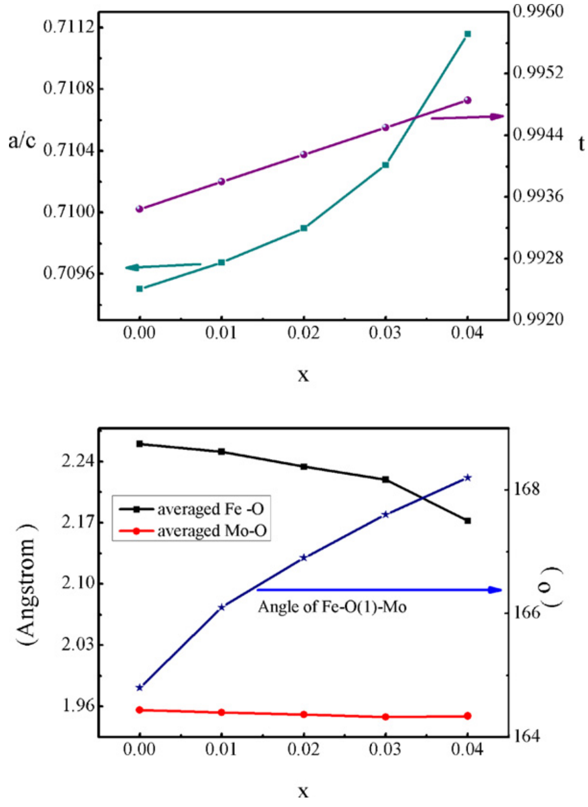

Fig. 2. (a) Tetragonal distortion of a/c (left) and the tolerance factor of t (right) versus the doping content x. (b) The bond length of Fe—O and Mo—O (left) as a function of x, the angle of Fe—O(1)—Mo (right) as a function of x.

The refinement is performed according to the group order as reported in references [23,24]. As an example, the refinement details are shown in Fig. 1(b) for $x = 0$. Refinement processes are smooth and the difference between the measured pattern and the calculated one is very small. The refinement reliability is ensured by the refinement parameter $R_{wp} = 5.68\%$, with lattice parameters $a = b = 5.5798(9)$ Å, and $c = 7.8645(1)$ Å. R_{wp} is in the range of 5–6% for all samples. The substitution of K^{1+} for Sr^{2+} ions induces the crystal lattice distortion although the crystal structure of all samples remains the tetragonal. The crystal lattice distortion, bond length, and bond-angle of Fe—O—Mo may be crucial for understanding the change in magnetic property in SFMO.

We obtain structure parameters from Rietveld refinements, and calculate the tetragonal distortion of a/c, as shown in Fig. 2 (a) left. a, c, and v, increase monotonously with increasing x, which can be interpreted by larger ion radius of K^{1+} substitution for Sr^{2+}. The values of a/c also increase monotonously with increasing x. The change of a/c leads us to recall of the tolerance factor t, defined as $t = \frac{r_A + r_O}{\sqrt{2}(r_B + r_O)}$, with r_A, r_B, and r_O are the ionic radii of A, B, and oxygen, respectively. The tolerance factor is a semi-quantitative estimation for the difference of the symmetry of an ABO_3 perovskite-like unit cell from the cubic one. A large deviation of t from 1 suggests that the perovskite structure may be unstable [25]. The tolerance factor concept can be adapted to double perovskites as well. In general, for double perovskites, with the mixed A site $A_{(2-x)}A'_xBB'O_6$, we may define the tolerance factor in this system

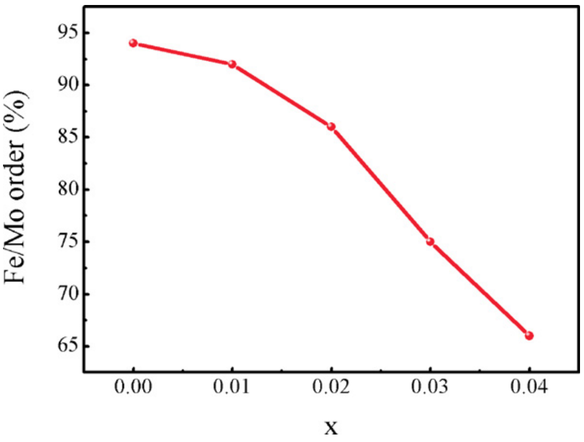

Fig. 3. The Fe/Mo order as a function of x.

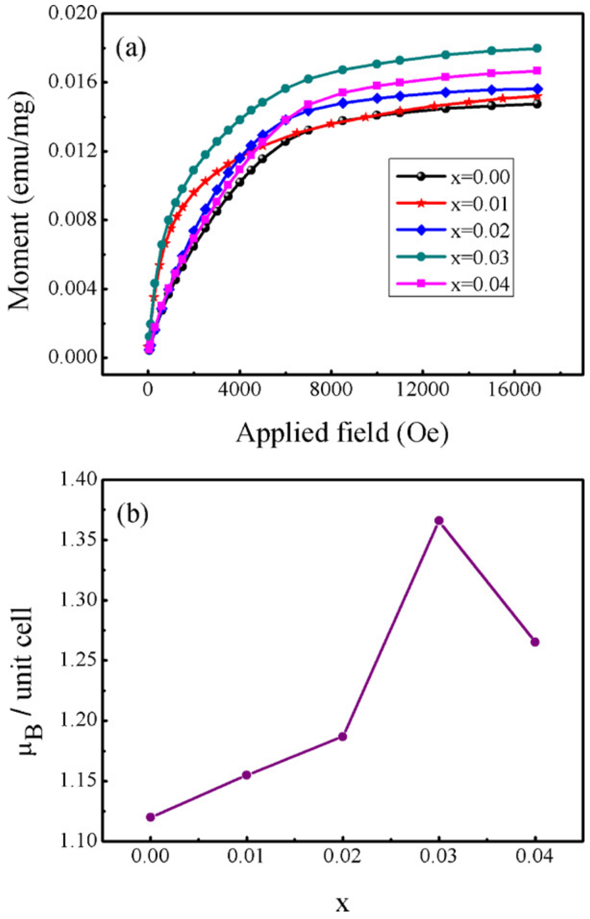

Fig. 4. (a) Magnetization curves of $Sr_{2-x}K_xFeMoO_6$ ($0 \le x \le 0.04$) at 280 K; (b) The dependence of unit cell magnetic moment on doping content x at 280 K.

as $t = \frac{1-(x/2)r_A+(x/2)r_{A'}+r_O}{\sqrt{2}((r_B/2)+(r_{B'}/2)+r_O)}$, where r_A, $r_{A'}$, r_B, $r_{B'}$ are the ionic radii of the respective ions. The ionic sizes for Sr^{2+}, K^{1+}, Fe^{3+}, Mo^{5+} and O^{2-} are 1.44 Å (coordination number, denote as CN, XII), 1.64 Å (CN, XII), 0.645 Å (CN, VI), 0.61Å(CN, VI), and 1.38Å(CN, IV), respectively [26]. The calculated dependence of t on x for $Sr_{(2-x)}K_xFeMoO_6$ is shown in Fig. 2(a) right. That the values of t and a/c increase monotonously with increasing x suggests that larger K^{1+} substitution of Sr^{2+} leads to enhancement of tetragonal symmetry. This coincides with reference [27] which indicates that symmetry will become up because of larger ion substitution in A-site.

Fig. 2 (b) shows bond lengths (left) and bond angles (right) vary with the concentration of K for $Sr_{2-x}K_xFeMoO_6$, which are obtained from Rietveld refinements using the XRD data above. The averaged Fe—O bond-length decreases with increasing K doping, which may indicate Fe supply more electrons to O in forming Fe—O bond. The averaged Mo—O bond-length remains almost unchanged after K doping. The variation in averaged bond-lengths of Fe—O and Mo—O seems confirming that: Fe may increase the valence state after K doping and Mo remain that unchanged. The angle of Fe—O(1)—Mo as a function of x is shown in Fig. 2(b) right. The double exchange and the super exchange are two different mechanisms for the magnetic relation between Fe and Mo ions. According to [18], the super exchange may be not suited to describe magnetic relation in SFMO and the double exchange may be the main explanations. The double exchange relates to the bond angle [8], which has a good exchange with the bond angle approaching 180°. The angle increases with increasing x suggests that the double exchange maybe enhance, which is one of important reasons for magnetic property in SFMO.

The occupancy of Fe at B-site and that of Mo at B′-site have been determined from Rietveld refinements. We define the cation-ordering η as $\eta = 1 - 2AS$, where AS is the occupancy of Fe at B′-site or Mo at B-site, which so called anti-site occupancy. The value of η decreases from 94.2(8)% for sample $x = 0$–66.1(2) % for sample $x = 0.04$, as shown in Fig. 3. The cation-ordering relates to the difference of the chemical valence between Fe and Mo ions [12]. The chemical valence of Fe and Mo may respectively be $Fe^{2+\delta}$ and $Mo^{6-\delta}$, with $\delta = \pm 1$. The substitution of K^{1+} for Sr^{2+} ions may induce the decrease of the chemical valence at A-site, which may be compensated by the increase of the chemical valence at B/B′-sites, i.e., the decrease of the chemical valence at Sr^{2+}/K^{1+} site results in the variation of the chemical valence of Fe or Mo. If the chemical valence of element Mo set as $6 - \delta$, the increase of chemical valence at B or B′-sites may result from the enhancement of Fe. The deduction is confirmed by the variation of the averaged bond-length of Fe—O and Mo—O. The less the valence difference is, the more disorder between Fe and Mo is.

Within the framework of the simplest ferromagnetic-arrangement model (the FIM model) and assuming a spin-only contribution, the moments of the Fe^{3+} and the Mo^{5+} sublattices are 5 μ_B/unit cell and 1 μ_B/unit cell, respectively, for a perfectly cation-ordering SFMO. The moments between the Fe^{3+} and the Mo^{5+} sublattices couple in antiferromagnetic, resulting in a saturation magnetization (M_S) of 4 μ_B/unit cell. However, Mössbauer spectroscopy studies have proved that a valence mixing of Fe and Mo appears in SFMO, i.e., the configurations of Fe^{2+}–Mo^{6+} and Fe^{3+}–Mo^{5+} [28]. The valence mixing configurations of Fe and Mo remains the M_S of 4 μ_B/unit-cell, which still fits the FIM model. The magnetization dependence on the applied magnetic field for each sample at 280 K is shown in Fig. 4(a). Based on the magnetization curves, we calculate the unit cell magnetization at 280 K, as shown in Fig. 4 (b). The magnetization is in the range of 1.12–1.26 μ_B/unit-cell at 280 K for all samples, which is much smaller than that at 5 K. We explain the magnetization decrease at high temperature is: (1) Thermal energy induces the spin-flip of partial Fe-ion, and disturbs the ferromagnetic-ordering among Fe-ions and Mo-ions. (2) Spin-orbit coupling interaction may play some roles on the magnetization in the system. The unit cell magnetization increases with increasing x when $x \le 0.03$, but decreases with increasing x when $x \ge 0.03$, as shown in Fig. 4(b). The Fe—O(1)—Mo bond-angle, the AS defect may have the competitive effects on the magnetization in the system. The Fe—O(1)—Mo bond-angle increases with increasing x, as studied by XRD and shown in Fig. 2(b), enhances the double exchange between Fe and Mo. The double exchange

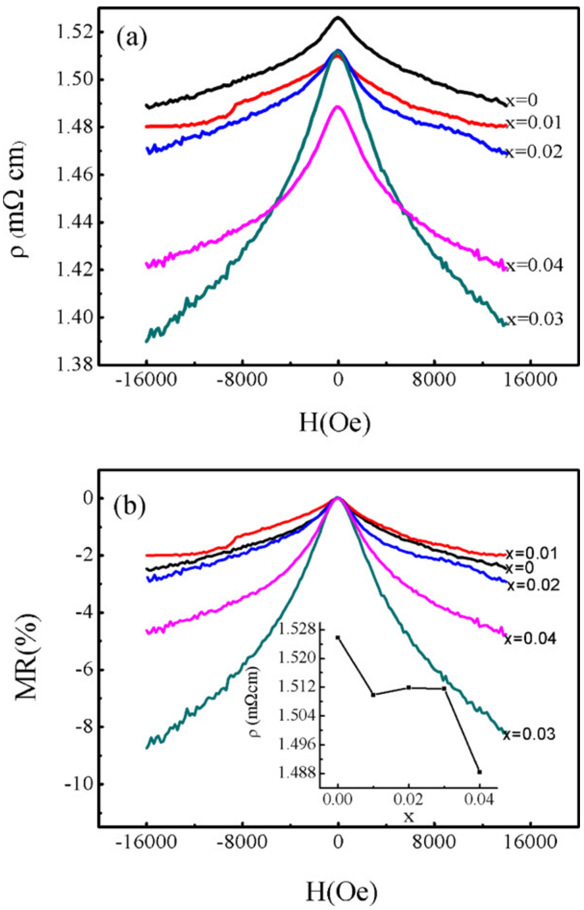

Fig. 5. (a) Field dependence of resistivity of $Sr_{2-x}K_xFeMoO_6$ ($0 \leq x \leq 0.04$) at 280 K; (b) Field dependence of magnetoresistance of the series at 280 K. Inset in (b) shows the resistivity at 280 K under zero field as a function of x.

interactions between Fe and Mo may play the main roles on the magnetization with $x \leq 0.03$. On the other hand, AS defects may destroy the ferromagnetic-ordering in SFMO compounds [29]. The antiferromagnetic configuration of Fe—O—Fe may increase with increasing the concentration of AS defects, which cripples the effect of the Fe-moment on the magnetization in the unit cell. The cation-ordering decreases from 94.2(8)% for sample $x = 0$–66.1(2)% for sample $x = 0.04$ (as shown in Fig. 3) and the AS defect increases from 2.8(6)% for sample $x = 0$ to 16.9(4)% for sample $x = 0.04$. AS defect possibly plays the main role on the magnetization in the sample with $x = 0.04$.

One of the most remarkable properties of polycrystalline SFMO is its large MR, which is usually explained by the intergrain spin-dependent carrier scattering process [30]. This explanation is based on the fact that the grain boundary resistance can be modulated by an applied magnetic field. The magnetoresistance is here defined to be: $MR(T, H) = \frac{\rho(T,H)-\rho(T,0)}{\rho(T,H)}$, where $\rho(T, H)$ and $\rho(T, 0)$ are the resistivity under a field of H and a zero field at temperature T, respectively. Fig. 5(a) shows field dependence of resistivity of $Sr_{2-x}K_xFeMoO_6$ ($0 \leq x \leq 0.04$) at 280 K. Inset in Fig. 5(b) shows the resistivity at 280 K as a function of x under zero magnetic field applied. According to Anderson and Hasegawa [31], transfer integral increases with increasing the bond-angle of Fe—O(1)—Mo. We note in the right of Fig. 2(b) that the bond-angle of Fe—O(1)—Mo increases with increasing x. Therefore, the increase of transfer integral may result in the decrease in resistivity, as shown in the inset of Fig. 5(b). The decrease of MR for sample with $x = 0.04$ (see in Fig. 5(b)) may explain as the increase of AS defect. The AS defect may indicate the existence of antiferromagnetic configuration of Fe—O—Fe patches in the system. The increase of AS defect concentration may extend the antiferromagnetic composition Fe—O—Fe patches, which may decrease the tunneling possibility for the spin-polarized carriers crossing the grain boundary based on the two-current model and leading to the lower MR of the compounds.

Conclusions

In summary, we successfully incorporate K into ordered double perovskite oxide Sr_2FeMoO_6. X-ray powder diffraction results show that all the samples are single phase. The substitution of K^{1+} for Sr^{2+} ions induces the lattice distortion although the unit cell symmetry of all samples remains I4/m. Symmetry becomes up because of larger ion substitution of A site. The averaged bond length of Fe—O and Mo—O confirms that the increase of chemical valence at B or B′ site may be from the raise in chemical valence of Fe-ion. The anti-site defect in double perovskite oxides of $Sr_{2-x}K_xFeMoO_6$ may be adjusted by alkali metal element of K doping. The unit cell magnetization at 280 K is 1.12 μ_B for $x = 0$ and 1.26 μ_B for $x = 0.04$, respectively. The cation-ordering, bond length, and bond-angle of Fe—O—Mo are crucial for understanding the change in magnetic property in SFMO.

Acknowledgement

This work is supported by the National Key Projects for Basic Researches of China (2010CB923404), the Natural Science Foundation of China (10974081, 10979017, and 11074066). The author Y.C. Hu is grateful for Henan Normal University Doctor Science Foundation (01026500109) and Henan Province Key Laboratory of Photovoltaic Materials. We are also in debt to Prof. Xiaoshan Wu, from the University of Nanjing, for his insightful comments.

References

[1] Y.W. Long, N. Hayashi, T. Saito, M. Azuma, S. Muranaka, Y. Shimakawa, Nature 458 (2009) 60–63.
[2] S. Chakraverty, K. Yoshimatsu, Y. Kozuka, H. Kumigashira, M. Oshima, T. Makino, A. Ohtomo, M. Kawasaki, Phys. Rev. B 84 (2011) 132411.
[3] A. Prodi, E. Gilioli, A. Gauzzi, F. Licci, M. Marezio, F. Bolzoni, Q. Huang, A. Santoro, J.W. Lynn, Nat. Mater. 3 (2004) 48–52.
[4] Yonatan Dubi, Yigal Meir, Yshai Avishai, Nature 449 (2007) 876–880.
[5] S. Yanez-Vilar, E.D. Mun, V.S. Zapf, B.G. Ueland, J.S. Gardner, J.D. Thompson, J. Singleton, M. Sanchez-Andujar, J. Mira, N. Biskup, M.A. Senaris-Rodriguez, C.D. Batista, Phys. Rev. B 84 (2011) 134427.
[6] K.-I. Kobayashi, T. Kimura, H. Sawada, K. Terakura, Y. Tokura, Nature 395 (1998) 677–680.
[7] F.K. Patterson, C.W. Moeller, R. Ward, Inorg. Chem. 2 (1963) 196–198.
[8] F.S. Galasso, F.C. Douglas, R.J. Kasper, J. Chem. Phys. 44 (1966) 1672–1674.
[9] Adam J. Hauser, Robert E.A. Williams, Rebecca A. Ricciardo, Arda Genc, Manisha Dixit, Jeremy M. Lucy, Patrick M. Woodward, Hamish L. Fraser, Fengyuan Yang, Phys. Rev. B 83 (2011) 014407.
[10] Raghava P. Panguluri, Sheng Xu, Yutaka Moritomo, I.V. Solovyev, B. Nadgorny, Appl. Phys. Lett. 94 (2009) 012501.
[11] B.-G. Park, Y.-H. Jeong, J.-H. Park, Phys. Rev. B 79 (2009) 035105.
[12] Mark T. Anderson, Kevin B. Greenwood, Gregg A. Taylor, Kenneth.R. Poeppelmeier, Prog. Solid State Chem. 22 (1993) 197–233.
[13] M. Imada, A. Fujimori, Y. Tokura, Rev. Mod. Phys. 70 (1998) 1039–1263.
[14] T. Goto, B. Luthi, Adv. Phys. 52 (2003) 67–118.
[15] P.A. Lee, N. Nagaosa, X.G. Wen, Rev. Mod. Phys. 78 (2006) 17–85.
[16] M.B. Salamon, M. Jaime, Rev. Mod. Phys. 73 (2001) 583–628.
[17] J. Navarro, J. Fontcuberta, M. Izquierdo, J. Avila, M.C. Asensio, Phys. Rev. B 69 (2004) 115101.
[18] Y.C. Hu, J.J. Ge, Q. Ji, Z.S. Jiang, X.S. Wu, G.F. Cheng, Mater. Chem. Phys. 124 (2010) 274–280.
[19] Y.C. Hu, Q. Ji, J.J. Ge, R.B. Xie, Z.S. Jiang, X.S. Wu, G.F. Cheng, Hairui Liu, Qingfeng Lu, J. Alloys Compd. 492 (2010) 496–499.
[20] B.H. Toby, J. Appl. Crystallogr. 34 (2001) 210–213.
[21] W.M. Chen, J. Chen, X. Jin, Physica C 276 (1997) 132–138.
[22] W.M. Chen, W. Hong, J.F. Geng, X.S. Wu, W. Ji, L.Y. Li, L. Qui, X. Jin, Physica C 270 (1996) 349–353.
[23] X.S. Wu, W.M. Chen, X. Jin, S.S. Jiang, Physica C 273 (1996) 99–106.

[24] X.S. Wu, S.S. Jiang, N. Xu, F.M. Pan, X.R. Huang, W. Ji, Mao Zhiqiang, Xu Gaoji, Zhang Yuheng, Physica C 266 (1996) 296–302.

[25] Min Feng LÜ, Jing Ping Wang, Jian Fen Liu, Wei Song, Xian Feng Hao, De Feng Zhou, Xiao Juan Liu, Zhi Jian Wu, Jian Meng, J. Alloys. Compd. 428 (2007) 214–219.

[26] R.D. Shannon, Acta Crystallogr. 32 (1976) 751–767.

[27] J.M. De Teresa, D. Serrate, J. Blasco, M.R. Ibarra, L. Morellon, Phys. Rev. B 69 (2004) 144401.

[28] J. Linden, T. Yamamoto, M. Karppinen, H. Yamauchi, T. Pietari, Appl. Phys. Lett. 76 (2000) 2925–2927.

[29] B. Ana, Muñoz-García, Michele Pavone, A. Carter Emily, Chem. Mater. 23 (2011) 4525–4536.

[30] K.I. Kobayashi, T. Kimura, Y. Tomioka, H. Sawada, K. Terakura, Y. Tokura, Phys. Rev. B 59 (1999) 11159–11162.

[31] P.W. Anderson, H. Hasegawa, Phys. Rev. 100 (1955) 675–681.